

# MedicoSAM: Towards foundation models for medical image segmentation

Anwai Archit, Luca Freckmann, Constantin Pape

**Abstract**—Medical image segmentation is an important analysis task in clinical practice and research. Deep learning has massively advanced the field, but current approaches are mostly based on models trained for a specific task. Training such models or adapting them to a new condition is costly due to the need for (manually) labeled data. The emergence of vision foundation models, especially Segment Anything, offers a path to universal segmentation for medical images, overcoming these issues. Here, we study how to improve Segment Anything for medical images by comparing different finetuning strategies on a large and diverse dataset. We evaluate the finetuned models on a wide range of interactive and (automatic) semantic segmentation tasks. We find that the performance can be clearly improved for interactive segmentation. However, semantic segmentation does not benefit from pretraining on medical images. Our best model, MedicoSAM, is publicly available. We show that it is compatible with existing tools for data annotation and believe that it will be of great practical value.

**Index Terms**—medical-imaging, segmentation, segment-anything, foundation-model, finetuning

## I. INTRODUCTION

Foundation models are large deep neural networks, often based on the transformer architecture [55], which are trained on diverse datasets, either using self-supervised or supervised training objectives. They learn powerful representations that enable different downstream tasks either through in-context learning or finetuning. They underlie recent advances in language processing [3] and are also gaining importance in computer vision, thanks to the vision transformer (ViT) [12]. The first foundation model that has gained wide-spread adoption for image segmentation is the Segment Anything Model (SAM) [28]. It was trained on a large dataset of natural images with object annotations, using a supervised training objective that mimics interactive annotation. The model supports interactive and automatic segmentation tasks and generalizes to many different imaging modalities. More recently, SAM2 [50] has extended SAM to video data through architectural changes and a large video dataset with objects tracked over time. It supports interactive video segmentation in different modalities.

SAM has been widely studied by the medical imaging community. Initial work has evaluated it for medical segmentation tasks (e.g. [46, 25, 18]). The model showed impressive performance given that it was predominantly trained on natural

images, but could not yet compete with domain specific models, especially for difficult tasks such as spine segmentation in MRI [46], segmentation of small organs in CT [22], and other examples [7, 18]. Consequently, follow-up work has improved SAM for medical images, either by finetuning it for interactive segmentation [40, 7, 56, 35] or by using it as a pretrained encoder for semantic segmentation [64, 58, 6, 16, 62, 4]. The model has also been adapted in related domains, for example to improve segmentation in microscopy [1] and histopathology [20]. Some work [40, 7, 16] also tried to build a better *foundation model for medical images*, by finetuning SAM on a large medical dataset and publishing the updated model weights. Preliminary studies have also investigated SAM2 for medical images [11, 65, 41]. They found mixed results for 2D segmentation, improving over SAM for some modalities but with worse performance for others, and promising results for video segmentation [36].

However, a comprehensive study that compares different approaches for improving SAM as a foundation model for medical images is so far missing. In particular, prior work has not yet considered different criteria such a model should fulfill together:

- 1) It should improve interactive segmentation. The imaging modalities and segmentation tasks in medicine are very diverse. Hence, a single model that can solve any medical segmentation task fully automatically is currently not feasible<sup>1</sup>. Better interactive segmentation will enable semi-automatic data annotation, leading to faster annotation times, either for data analysis or model training.
- 2) It should improve the performance for downstream tasks, in particular as a pretrained encoder for semantic segmentation. This would enable fully automating segmentation tasks by supervised finetuning; potentially using annotations generated interactively via (1).
- 3) It should be compatible with the original SAM library and graphical data annotation tools that use it (e.g. [37, 1]), enabling users to benefit from improved interactive segmentation (1).

Previous work has only addressed one of these aspects at a time: MedSAM [40] and SAMed2D [7] only evaluate interactive segmentation (1), Gu et al. [16] only study semantic segmentation (2). They do not explicitly study use of their

<sup>1</sup>There exist some efforts to establish such models for specific modalities, most notably TotalSegmentator [57, 10] for CT and MRI images.

models in user-friendly tools (3), and we find that only MedSAM is compatible with them.

Our work closes this gap by comparing different training approaches on the dataset published by SAMed2d [7] and evaluating their efficacy for (1-3). Specifically, we compare different interactive-style finetuning approaches using our own implementation as well as extant SAM-based models. We compare these models for challenging medical segmentation tasks from four different categories: (i) interactive 2D segmentation, (ii) interactive 3D segmentation, (iii) semantic 2D segmentation, and (iv) semantic 3D segmentation. Where applicable, we also compare to SAM2, though we do not finetune it for medical data due to the recent release of this model and the lack of support in user-friendly tools. An overview of our approach is shown in Fig. 1 a) and the summary of our evaluation results is shown in Fig. 1 b-e). Overall, we find that domain specific finetuning can clearly improve interactive segmentation in 2D and 3D, given the right training objective. For semantic segmentation, finetuning does not provide a clear advantage as models pretrained on medical images do not consistently improve over the original SAM model. We also find that SAM-based architectures for semantic segmentation are not consistently better than nnU-Net [23]. Our code and our best model, which we call MedicoSAM, are available at <https://github.com/computational-cell-analytics/medico-sam>.

## II. METHODS

We provide a summary of the contributions made by SAM, focusing on its training objective (Sec. II-A). We then describe the finetuning approaches used in our study (Sec. II-B), the extension of SAM to interactive 3D segmentation (Sec. II-C), the methods for 2D and 3D semantic segmentation (Sec. II-D), and our evaluation methodology (Sec. II-E). We use these methods to compare different strategies to improve SAM for medical images and to train and publish MedicoSAM.

### A. Segment Anything

SAM [28] is a vision foundation model for segmentation tasks. It consists of the image encoder, a ViT [12], the prompt encoder and the mask decoder. This architecture enables the model to solve interactive segmentation tasks based on user input, so called prompts. The image encoder processes the image and outputs an image representation. It contains the majority of parameters. SAM provides three different versions with different encoder sizes, ViT-Huge (ViT-h), ViT-Large (ViT-l) and ViT-Base (ViT-b). The prompt encoder processes the prompts, which can be point coordinates, either a positive point prompt (within the object of interest) or a negative point prompt (outside of the object of interest), a box coordinate, or a low-resolution mask. It outputs a representation of the prompts; point, box and mask prompts can be combined. The mask decoder processes the outputs of image encoder and prompt encoder to predict a mask of the object of interest and a score that estimates the prediction quality. It has two heads. One predicts a single mask and score, the other predicts three masks and scores. The second head is for the case of a

single point prompt, which can result in ambiguities for part-object segmentation. Fig. 2 a) shows an overview of SAM's architecture.

SAM was evaluated for a wide range of segmentation tasks in diverse image modalities, where it showed remarkable generalization. These capabilities are mainly due to two factors: the large and diverse training set and the sophisticated training objective. The training dataset, which is called SA-1B, consists of eleven million images with one billion annotated objects. It was generated by human annotators using SAM for semi-automatic annotation, followed by retraining and further annotation with the updated model. This procedure was repeated multiple times. The model was trained on this dataset using a supervised training objective that mimics interactive object annotation and correction: For a given ground-truth mask, the objective first samples either a point or box prompt and then corrects the model predictions with point prompts in multiple steps. In each step it computes  $L_{mask}$ , the loss between true and predicted mask as well as  $L_{iou}$ , the loss between the intersection over union (IOU) of true and predicted mask and the predicted score. These losses are accumulated and averaged at the end of a training iteration. See Alg. 1 for the pseudo-code of a training iteration. Besides this objective, the training proceeds as usual for deep neural networks by updating model weights with a version of stochastic gradient descent over multiple epochs.

Recently, SAM was extended to videos by SAM2 [50]. This works extends the architecture with a memory bank to store prompts and mask predictions from previous frames, enabling interactive video segmentation. SAM2 was trained on a large annotated video dataset. While SAM2 is promising in the medical domain to analyze videos or volumetric data, it has so far received fewer attention. Initial studies [41, 11, 65] have evaluated it for this domain and also performed preliminary transfer learning experiments, but so far have not provided an improved SAM2 model for medical data. Here, we include SAM2 in the evaluation of interactive segmentation, but do not finetune the model on medical data due to its recency and missing support in tools for medical data annotation.

### B. Finetuning Segment Anything

We implement and compare different approaches for finetuning SAM to improve it for medical images. These approaches start by assembling a large labeled dataset of medical images and finetuning SAM on it using a variation of Alg. 1. The training algorithm has not been published by [28], so each publication has used a custom implementation. The finetuning strategies also differ in which model parts they update, and whether an adapter-based strategy like LoRA [21] is used.

The authors of MedSAM [40] assemble a dataset of ca. 1.5 million masks from CT, Endoscopy, MRI, X-Ray and other modalities, based on previously published data. They introduce a simple training objective that uses only box prompts, which are derived during training from the mask annotations. This objective corresponds to setting  $n_{steps} = 0$ ,  $p_{box} = 1$ ,  $p_{mask} = 0$  in Alg. 1. They use SAM with ViT-b encoder and update all parameters of the image encoder

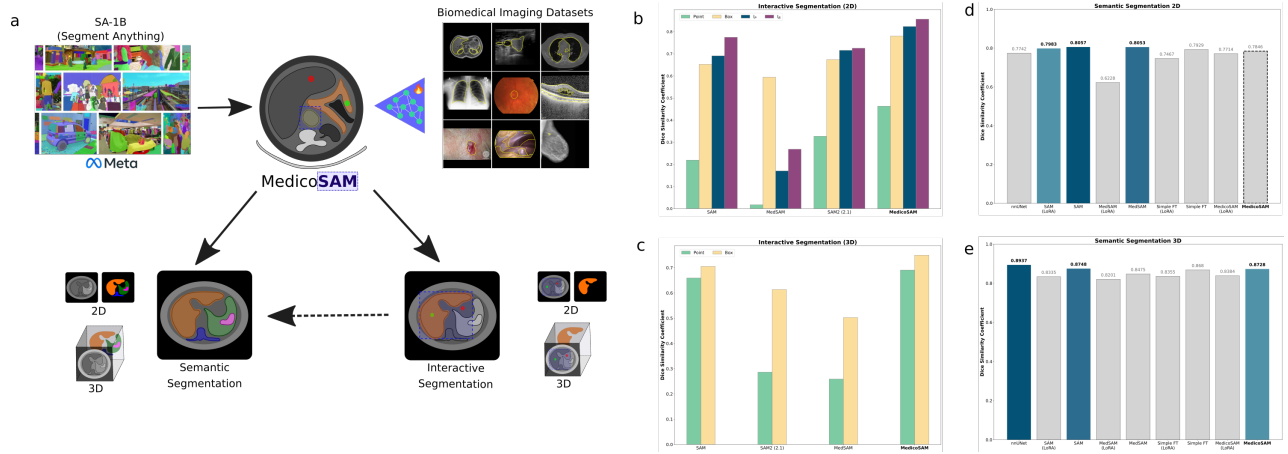


**Fig. 1.** **a)** Contribution overview: We finetune SAM on a large medical dataset to build MedicoSAM. We evaluate it for interactive segmentation and semantic segmentation, which requires training on additional annotated data (that could be generated via interactive segmentation), for 2D and 3D data. **b)** Results for interactive 2D segmentation, comparing MedicoSAM and other models derived from SAM. We report the average over 16 datasets for initial segmentation with a point (green) or box (yellow) and segmentation after iterative correction starting from a point (dark green) or box (dark purple). **c)** Results for interactive 3D segmentation. We report the average over 6 different datasets for segmentation based on a single point or box. **d, e).** Results for semantic 2D and 3D segmentation. We report the average over 6 datasets in both cases. The three best methods are highlighted, with MedicoSAM indicated by a dashed outline if it is not among the best models.

and mask decoder, freezing parameters of the prompt encoder. The finetuned model is evaluated for interactive segmentation based on box prompts. The model is publicly available.

The authors of SAM-Med2D [7] build the SA-Med2D-20M dataset [59], which consists of ca. 20 million masks in ca. 5 million images. The data covers ten different modalities (CT, Endoscopy, MRI, ultrasound, X-Ray and others) and is collected from published data. They finetune using the full training objective with  $n_{steps} = 8$ ,  $p_{box} = 0.5$ ,  $p_{mask} = 1$ . However, they deviate from Alg. 1 in two ways: they sample either 1, 3, 5 or 9 points per step instead of a single positive and negative one (cf. lines 23-24) and they do not compute gradients for the prompt encoder in the steps corresponding to lines 22-29. They use ViT-b and update the parameters of all model parts. They use a custom adapter for the image encoder, similar to [58], where a low rank projection layer is inserted between attention and feed-forward layer of each transformer block. Only the parameters of this layer are updated during training, the others are frozen. In addition, they train the model with a smaller input image size of 256 x 256 pixels instead of 1024 x 1024 pixels used by SAM. They also study a simpler finetuning strategy called FT-SAM where only the mask decoder is updated during training, image and prompt encoder are frozen. The finetuned models are evaluated for interactive segmentation and are publicly available.

The authors of [16] assemble a dataset for finetuning comprising ca. 100,000 masks in ca. 300,000 images from CT, MRI, X-Ray and ultrasound. This dataset also contains unlabeled images that are used for self-supervised training. They compare two different finetuning objectives: updating the image encoder in a self-supervised manner using MAE [17] and using a simple supervised strategy with a box or a single point prompt, corresponding to  $n_{steps} = 0$ ,  $p_{box} = 0.5$ ,  $p_{mask} = 0$  in Alg. 1. They further compare finetuning the different model sizes with and without the use of LoRA [21]. They evaluate these models for semantic segmentation

downstream tasks. None of the models are publicly available.

In summary, prior work has studied different finetuning objectives and different model update strategies. To study the influence of the objectives we build on the flexible implementation of Alg. 1 provided by  $\mu$ SAM [1], which was developed for microscopy data. We extend this implementation to also support simpler schemes (single box prompt / single box and point prompt) within the same framework. We do not study self-supervised training and finetune all model parts without the use of adapter layers. The first choice is due to the fact that self-supervised training would very likely lead to a loss of interactive segmentation performance. The second choice because we want to provide models that are compatible with the SAM library and tools using it. Introducing adapter layers would make the model incompatible and thus not practically useful, see also Sec. III-C. Consequently, we study three different finetuning strategies:

- MedSAM\* (adapted from [40]) uses only a box prompt, corresponding to  $n_{steps} = 0$ ,  $p_{box} = 1$ ,  $p_{mask} = 0$  in Alg. 1.
- SimpleFT\* (adapted from [16]) uses a single box or a single point prompt, corresponding to  $n_{steps} = 0$ ,  $p_{box} = 0.5$ ,  $p_{mask} = 0$  in Alg. 1.
- MedicoSAM uses the full objective with  $n_{steps} = 8$ ,  $p_{box} = 0.5$ ,  $p_{mask} = 0^2$ .

The parameter  $n_{obj}$  is set to five for all three cases and we use the Dice loss for  $L_{mask}$  and the L2 loss for  $L_{iou}$ . We finetune these three models on SA-Med2D-20M [59]. We also benchmark the published models MedSAM [40], SAM-Med2D [7], FT-SAM [7], SAM [28], and where applicable SAM2 [50]. We use ViT-b for all models.

<sup>2</sup>We use  $p_{mask} = 0$  for parallel training on multiple GPUs. As a consequence, this model should be used without mask prompts. We performed initial experiments with a model trained with  $p_{mask} = 0.5$  found that omitting mask prompts in interactive segmentation has no negative effect.

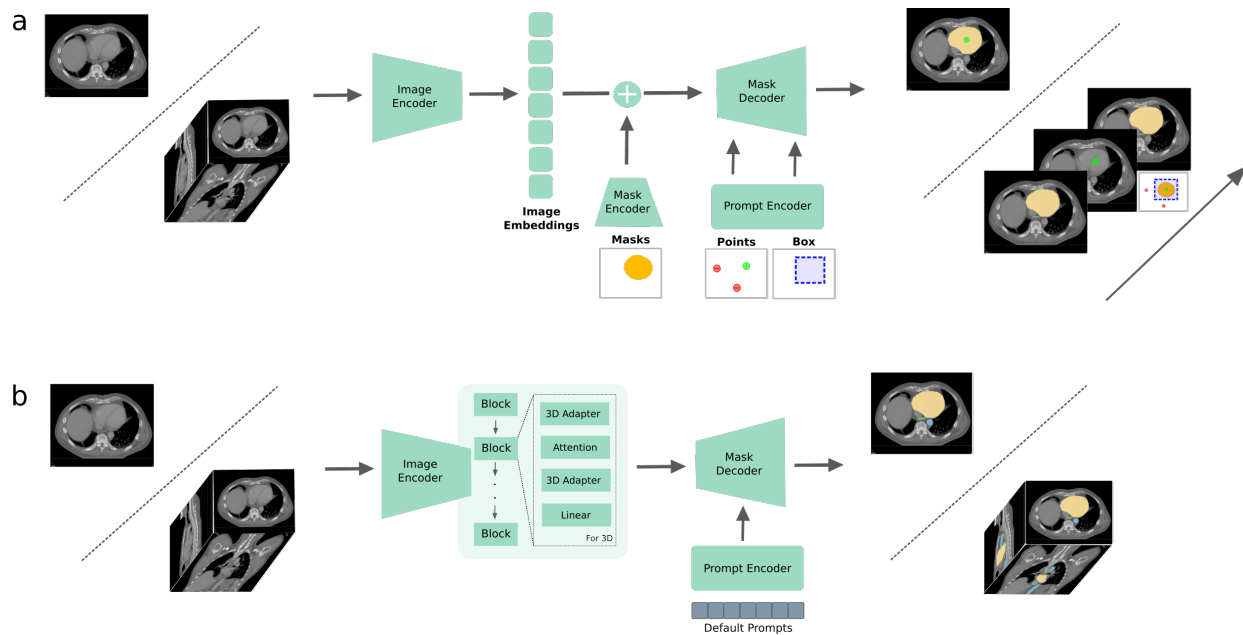


**Fig. 2.** **a)** The SAM architecture for interactive segmentation consists of image encoder, prompt encoder (split into a part for mask prompts and a part for point/box prompts) and mask decoder. **b)** Adaptation for semantic segmentation following [64] (2D) and [6] (3D). User prompts are replaced with a learnable prompt. The mask decoder is repurposed to predict the semantic segmentation. For 3D segmentation patch tokens across the depth axis are processed by additional 3D convolutions inserted in the image encoder.

### C. Interactive 3D Segmentation

Unlike SAM2, which supports image and video segmentation, SAM supports segmentation only for 2D data. Follow-up work has implemented interactive segmentation for videos or volumetric data in medical images, e.g. for CT [34] and Bone CT [43]. Here, we use the implementation from [1], which is based on prompt propagation. Briefly, a user annotates an object in one or multiple slices with prompts and SAM is applied to these slices. Then, the segmentation mask(s) are projected to adjacent slices, prompts are derived from them, and segmentation is run for these prompts. The process is repeated until the object is segmented throughout the whole volume or a stopping criterion based on the IOU between adjacent slices is met. Multiple options are provided for deriving prompts from projected masks: using a single positive point prompt placed at the mask’s center, using multiple point prompts derive from the mask, using the bounding box derived from the mask, using the bounding box and low-resolution version of the mask, and combinations of these options. A user can correct the segmentation by annotating slices with manual prompts and rerunning the segmentation.

### D. Semantic Segmentation

On its own, SAM can only be used for interactive segmentation. In [28] a method for automatic instance segmentation, called automatic mask generation, is proposed. However, this method only supports automatic instance segmentation and not semantic segmentation, which is the more relevant task for medical images. Conceptually, SAM does not learn explicit semantic knowledge, since it is only trained to distinguish objects without class information. Most approaches for semantic segmentation in medical images build on the U-Net [52,

8], nnU-NET [23] being the most popular one. To evaluate different pretrained SAM models for semantic segmentation, we finetune them for specific tasks using annotated data. We implement an architecture for 2D segmentation and one for 3D segmentation, see also Fig. 2b.

For 2D segmentation we implement SAMed [64]. It updates the SAM architecture by replacing input prompts with a learnable default prompt and changing the number of heads in the multi-mask decoder branch from three to the number of classes. The resulting model can be trained for semantic segmentation by updating parameters based on a loss between labels and predictions. We use the combination of Cross Entropy and Dice loss. Note that SAMed uses LoRA [21] in the image encoder. We compare two approaches, updating all parameters of the image encoder or using LoRA.

For 3D segmentation we implement MA-SAM [6]. This approach follows a similar design as SAMed, introducing additional changes to the image encoder. It flattens batch and depth dimension so that all image patches are processed by the transformer blocks. To make use of depth information it introduces 3D adapter layers. These layers decrease the number of features per token, rearrange tokens into a volumetric representation, apply a  $3 \times 1 \times 1$  convolution, project the number of features back and flatten the batch and depth axis. Each transformer layer is augmented with two of these adapters, one before the attention layer and the other after it. The parameters of the 3D adapters are randomly initialized and updated during training. The other parameters in the attention layers are either all updated or updated through LoRA (same as for 2D).

### E. Evaluation

We compare models for interactive and semantic segmentation. For semantic segmentation (2D and 3D), we follow stan-

**Algorithm 1:** The training objective of SAM. This pseudo-code describes the open-source implementation from [1], which slightly differs from [28].

---

**Input:** Images and ground-truth annotations,  
hyperparameters  $n_{obj}, n_{steps}, p_{box}, p_{mask}$   
**Output:** Updated model parameters

- 1 Sample minibatch of images and ground-truth
- 2 Sample fixed number of object masks  $n_{obj}$  per image
- 3 Predict embeddings for the images with the encoder
- 4 Initialize empty list  $L$  for losses
- 5 **for** mask  $m$  in minibatch **do**
- 6     Initialize empty list for prompts  $p$
- 7     Sample  $u_{box}$  uniformly from  $[0, 1]$
- 8     **if**  $u_{box} < p_{box}$  **then**
- 9         // The box can also be distorted
- 9         Compute bounding box of  $m$ , add as prompt to  $p$
- 10    **else**
- 11         Sample random point from  $m$ , add as as positive point prompt to  $p$
- 12    Apply prompt encoder to  $p$
- 13    **if**  $p$  contains single point prompt **then**
- 14         Predict masks and IOUs with multi mask head of mask decoder
- 15         Select predicted mask  $\hat{m}$  and IOU  $\hat{i}$  with the highest IOU value
- 16    **else**
- 17         Predict mask  $\hat{m}$  and IOU value  $\hat{i}$  with single mask head of mask decoder
- 18    Compute mask loss  $L_{mask}(\hat{m}, m)$
- 19    Compute IOU  $i$  between  $\hat{m}$  and  $m$
- 20    Compute regression loss  $L_{iou}(\hat{i}, i)$
- 21    Add  $L_{mask}$  and  $L_{iou}$  to  $L$
- 22    **for**  $j = 1$  to  $n_{steps}$  **do**
- 23         Sample positive point from  $m$  &  $\hat{m}$ , add to  $p$
- 24         Sample negative point from  $\neg m$  &  $\hat{m}$ , add to  $p$
- 25         Sample  $u_{mask}$  uniformly from  $[0, 1]$
- 26         Remove mask prompt from  $p$  if present
- 27         **if**  $u_{mask} < p_{mask}$  **then**
- 28             Add  $\hat{m}$  to  $p$
- 29         Run lines 12-21 with current  $p$
- 30 Average losses in  $L$ , perform backprop
- 31 Update model parameters via optimizer

---

dard procedures and compare the predicted semantic masks with ground-truth annotations using the Dice coefficient.

For interactive 2D segmentation we adopt the evaluation procedure of [1]. This approach simulates iterative user-based annotation. It requires object mask annotations. For a given object, a single prompt is sampled, either a point or a box. The object is then iteratively corrected by sampling point prompts from errors in the prediction. In each iteration a positive point prompt is sampled from the region where the prediction is missing (prediction is negative, annotation is positive) and a negative point prompt is sampled from the region where the prediction should not be (prediction is positive, annotation is negative). The Dice coefficient between true mask and prediction is computed for the initial segmentation and each correction iteration. For interactive 3D segmentation we evaluate the initial segmentation derived from a point prompt (randomly sampled from the object in the central slice) and

from a box prompt (also in the central slice). We do not simulate iterative correction of the masks due to the higher computational demand of 3D segmentation. We run a grid search over the different options for deriving prompts, see Sec. II-C, on separate validation data.

### III. EXPERIMENTS

We finetune three models based on SAM ViT-b, initialized with the weights from [28]: MedSAM\*, SimpleFT\* and MedicoSAM, see Sec. II-B for an explanation of the three different training set-ups. The three models are trained on the publicly available subset of SA-Med2D-20M [59], which contains 3,7 million images and 15,8 million masks. We use 50% of this dataset for training and 10% for validation, with a stratified split over the different modalities in the dataset. The remaining 40% of the dataset are not used to lower the training time per epoch. The models are trained on 8 A100 GPUs with 80GB VRAM for 300,000 iterations with a batch size of 7 per GPU, corresponding to 9 epochs. We use the AdamW optimizer [38] with an initial learning rate of  $5e - 5$  and a scheduler that reduces the learning rate by a factor of 0.9 after each epoch.

We evaluate these models and compare to the original SAM model and already published models for medical images for five different applications: interactive segmentation (2D and 3D), finetuning for semantic segmentation (2D and 3D) and integration with user-friendly tools.

#### A. Interactive Segmentation

We evaluate eight different models for interactive 2D segmentation, three we have finetuned and five published ones (including the original SAM and SAM2), see Sec. II-B for details. We use 16 *external* datasets that are not part of our training dataset to evaluate generalization capabilities. These datasets represent a variety of medical segmentation tasks from CT [48, 2, 49], dermoscopy [13], endoscopy [53, 44], MRI [42, 15], ophthalmology [29], ultrasound [32, 39, 27], and X-Ray [24, 33, 5, 63]. Here, 3D dataset are split into separate images.

The results averaged over all datasets are shown in Fig. 3 a). We report the results for initial prompt-based segmentation and correction iterations, see also Sec. II-E, using a point or box as initial prompt. Fig. 3 b) shows the results for all individual datasets, where we only report the results for the initial and final segmentation, corresponding to the last correction iteration. We report the difference in the Dice coefficient compared to SAM. Here, MedicoSAM is the only model that clearly improves upon SAM for all settings. The other finetuned models either only improve for the initial segmentation (MedSAM\*, SimpleFT\*) or lead to an overall worse segmentation performance. SAM2 performs slightly worse compared to (original) SAM. A qualitative comparison of model predictions is shown in Fig. 7 (supp. material).

We evaluate interactive 3D segmentation for the initial segmentation derived from a point prompt or a box prompt for 6 different external datasets from MRI [47, 42], CT [19, 54], and ultrasound [27, 30]. We compare five different models. For the models based on SAM, we use the method described in Sec. II-C and we find the best setting with a grid

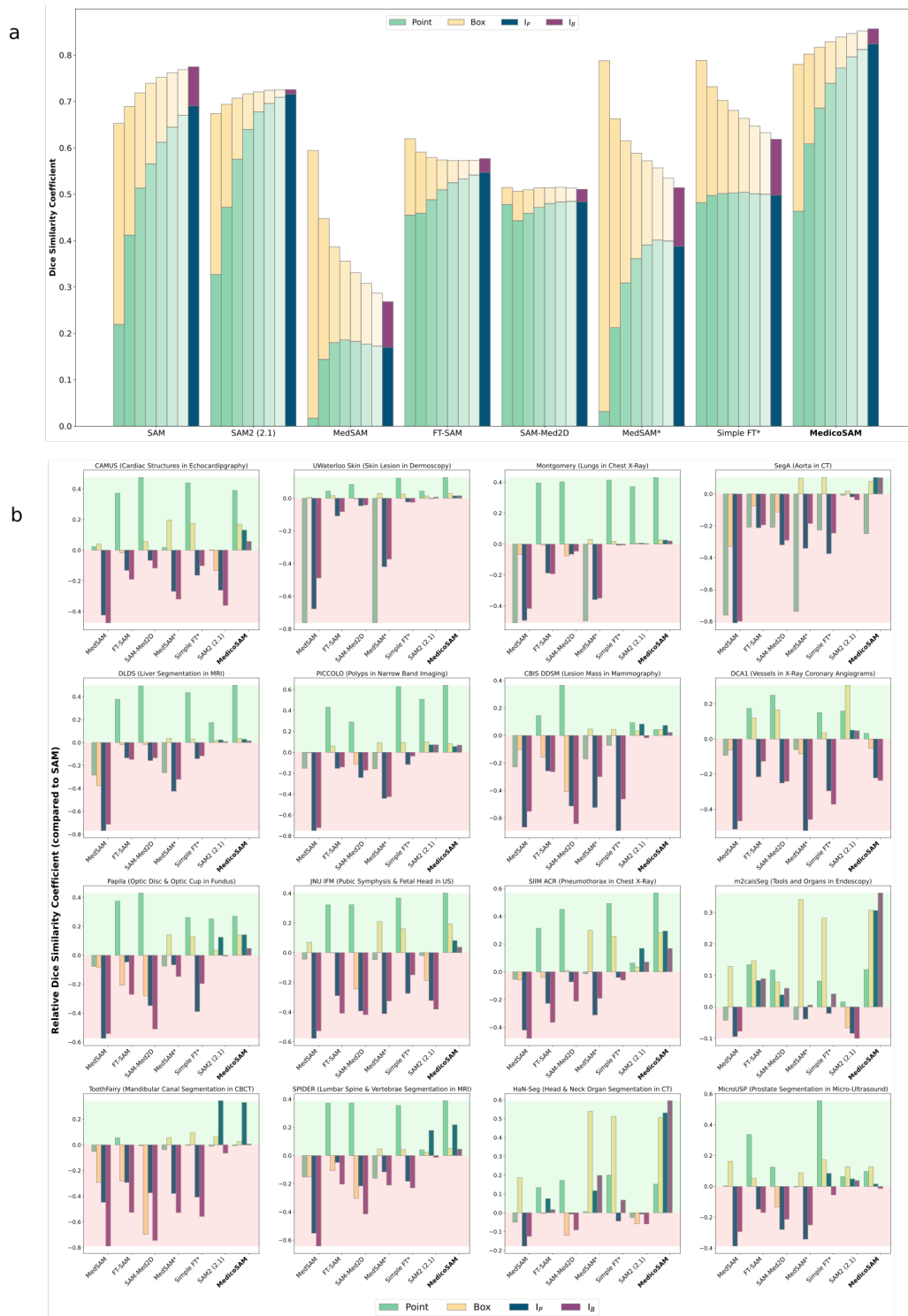


**Fig. 3.** **a)** Overall results for interactive 2D segmentation. We report the Dice coefficient for simulated interactive segmentation. Each bar corresponds to the result of a correction iteration, starting either from a point (green) or a box (yellow) prompt. The result after correction is highlighted in dark green / dark purple. We compare 8 different models. Models that were trained by us are marked with a \* or in bold for the MedicoSAM model. **b)** Interactive segmentation results for 16 individual datasets. We report the absolute difference of the Dice coefficient compared to the original SAM and report only the results for the initial and final segmentation.

search on a separate validation set. SAM2 supports interactive 3D segmentation as is (by interpreting the 3D data as a video), and we do not perform a grid search to optimize parameters for inference. The overall results are shown in Fig. 1 c) (except for SimpleFT) with results for individual datasets in Fig. 4.

Only MedicoSAM improves consistently. The fact that SAM2 is used as is, without optimizing parameters in a grid search, may disfavor it. A qualitative comparison of model predictions is shown in Fig. 8 (supp. material).

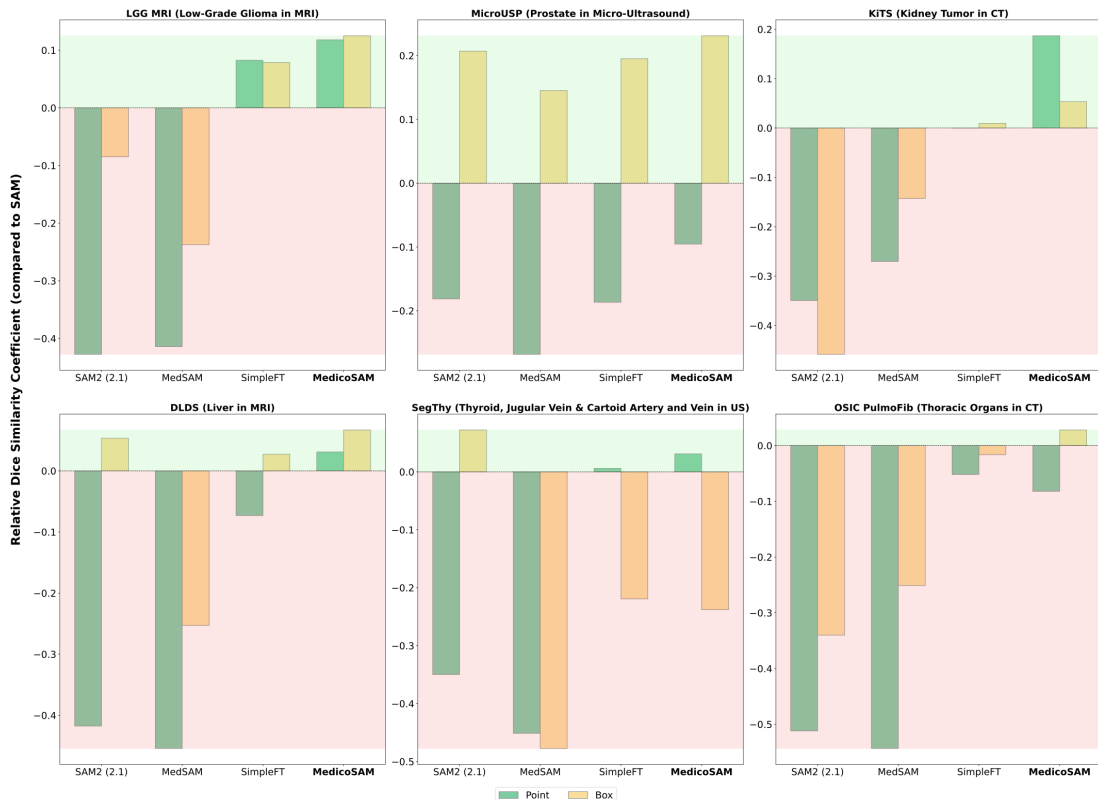


Fig. 4. Results for interactive 3D segmentation for 6 different datasets. We report the difference in Dice score compared to SAM for four other models. Segmentations are derived from a single point (green) or box (yellow) prompt placed in the central slice for each object in the respective dataset. We use the implementation of [1] for methods using SAM, determining the best method for prompt propagation on a separate validation set, see also Sec. II-C. SAM2 supports 3D segmentations by default.

## B. Semantic Segmentation

We evaluate the use of different pretrained SAM models for semantic segmentation in 2D and 3D, using the implementations described in Sec. II-D. We compare updating all parameters in the image encoder with parameter updates using LoRA [21]. For 2D segmentation we use 6 external datasets from dermoscopy [9], mammography [33], narrow band imaging [53], optical coherence tomography [60], panoramic radiographs [51], and X-Ray angiography [5]. For 3D segmentation we use 6 external datasets from CT [54], MRI [42, 45, 47], and ultrasound [27, 30]. We use separate splits for training and evaluation. The results are shown in Fig. 5. We also report the results for nnU-Net [23] trained on the training split of the respective dataset, using the default nnU-Net v2 setup.

Here, we do not see an advantage in using a domain-specific pretrained backbone (MedSAM, SimpleFT, MedicoSAM) over the initial SAM model. The architectures initialized with SAM weights perform on par or slightly better than initialization with these models. Furthermore, we don’t see a clear advantage in the use of SAM-based semantic segmentation compared to nnU-Net. While their performance is better overall in 2D, due to the poor performance of nnU-Net on two of the datasets, nnU-Net is the best method for 3D segmentation. Here, we have to stress that this comparison disfavors nnU-Net by design, as it is always trained from scratch, whereas the other methods are initialized with pretrained encoders. Finally, we find that results with LoRA are always slightly worse

compared to updating all parameters in the image encoder.

## C. Tool Integration

An important practical aspect in improving SAM as a foundation model for medical images is the integration with graphical tools for data annotation. Hence, models should not introduce changes to the SAM architecture that make the model incompatible with the SAM library and tools using it. We check this for three models, MedSAM, SAM-Med2D and MedicoSAM, and four different tools: two napari plugins [14, 1] and two 3D Slicer extensions [37, 61]. Tab. I shows the compatibility. We find that SAM-Med2D does not work in any of the tools because it uses adapters and changes the image input size. MedSAM and MedicoSAM work in all of the tools with at most small code changes. We qualitatively compare the models for data annotation with these tools in Fig. 6.

Tool / Model	MedSAM	SAM-Med2D	MedicoSAM
SegmentWithSAM	✓	✗	✓*
SAMM	✓	✗	✓*
napari-sam	✓	✗	✓*
μSAM	✓	✗	✓

TABLE I

COMPATIBILITY WITH USER-FRIENDLY TOOLS, FOR THREE MODELS AND FOUR GRAPHICAL TOOLS SUPPORTING SAM FOR DATA ANNOTATION. THE \* REPRESENTS MINOR CODE CHANGES NECESSARY TO ADAPT A FILE PATH OR URL TO LOAD DIFFERENT WEIGHTS.

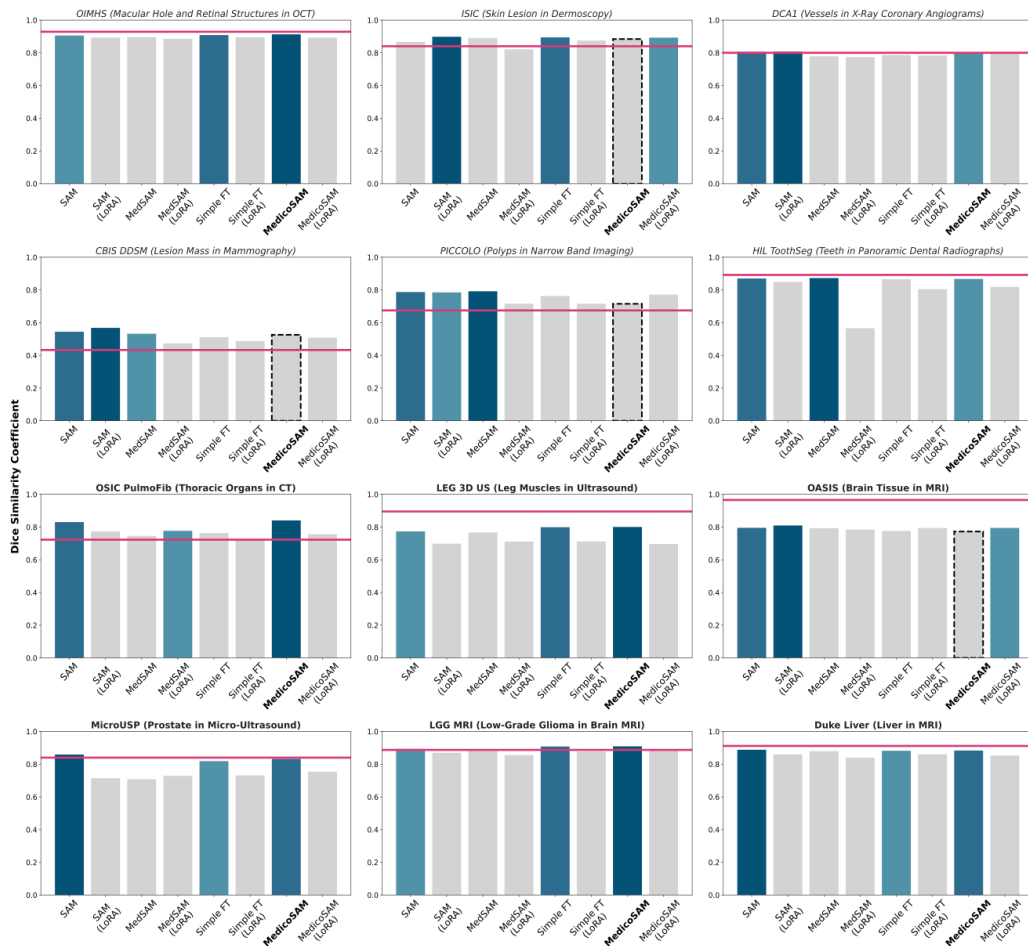


Fig. 5. Semantic segmentation results. We train an architecture for 2D and 3D segmentation. The names in italic font indicate 2D data and in bold font 3D data. We compare different pretrained models, original SAM, MedSAM, SimpleFT SAM, and MedicoSAM. We also compare updating all parameters of the encoder with LoRA. The three best methods are colored, in case MedicoSAM is not among them it is marked with a dashed outline. The red line marks the nnU-Net result.

#### IV. CONCLUSION

We have presented a comprehensive study of SAM for medical images, by evaluating the impact of different finetuning objectives on interactive segmentation and semantic segmentation. We found that interactive segmentation can improve clearly due to domain specific finetuning, compared both to original SAM and SAM2. In this context, the choice of the objective is crucial, and only the complex objective used in SAM preserves interactive segmentation capabilities, whereas simpler objectives as used in [40, 16] lead to diminishing capabilities for *iterative* interactive segmentation. For semantic segmentation we find that using a domain specific backbone does not provide a clear benefit, at least using the approaches we study. Further, we don't see a clear advantage of SAM-based architectures over nnU-Net [23]. Finally, we show that models based on SAM should adhere to the original architecture to enable integration within existing tools. We believe that this fact is especially important since, according to our findings, their main advantage is improved interactive data annotation, which relies on such tools.

Our contribution provides important updates to prior work on SAM for medical images. In [40], the authors claim

that their model, MedSAM, improves interactive segmentation when using a simple finetuning objective using only box prompts. However, according to our results, this only holds true for annotation from bounding boxes, and the model loses the capability for correction with additional prompts. Given that this capability is one of the main strengths of SAM, we believe that this leads to a worse model for practical applications; [40] misses this observation due to a simplistic evaluation procedure that only evaluates box prompts. While SAM-Med2D [7] uses a comprehensive finetuning objective and evaluation procedure, it uses adapters and changes the input image size, making it incompatible with existing tools. In [16], the authors study SAM as basis for semantic segmentation. In addition to finetuning with a prompt-based objective, they also study self-supervised finetuning. They find that prompt-based finetuning does not improve the performance for downstream semantic segmentation, which is consistent with our results, and that self-supervised finetuning may be slightly beneficial (we do not study this setting, because it will very likely lead to catastrophic forgetting of interactive segmentation capabilities). Furthermore, they claim that finetuning SAM shows advantages over nnU-Net, and that LoRA-based updates



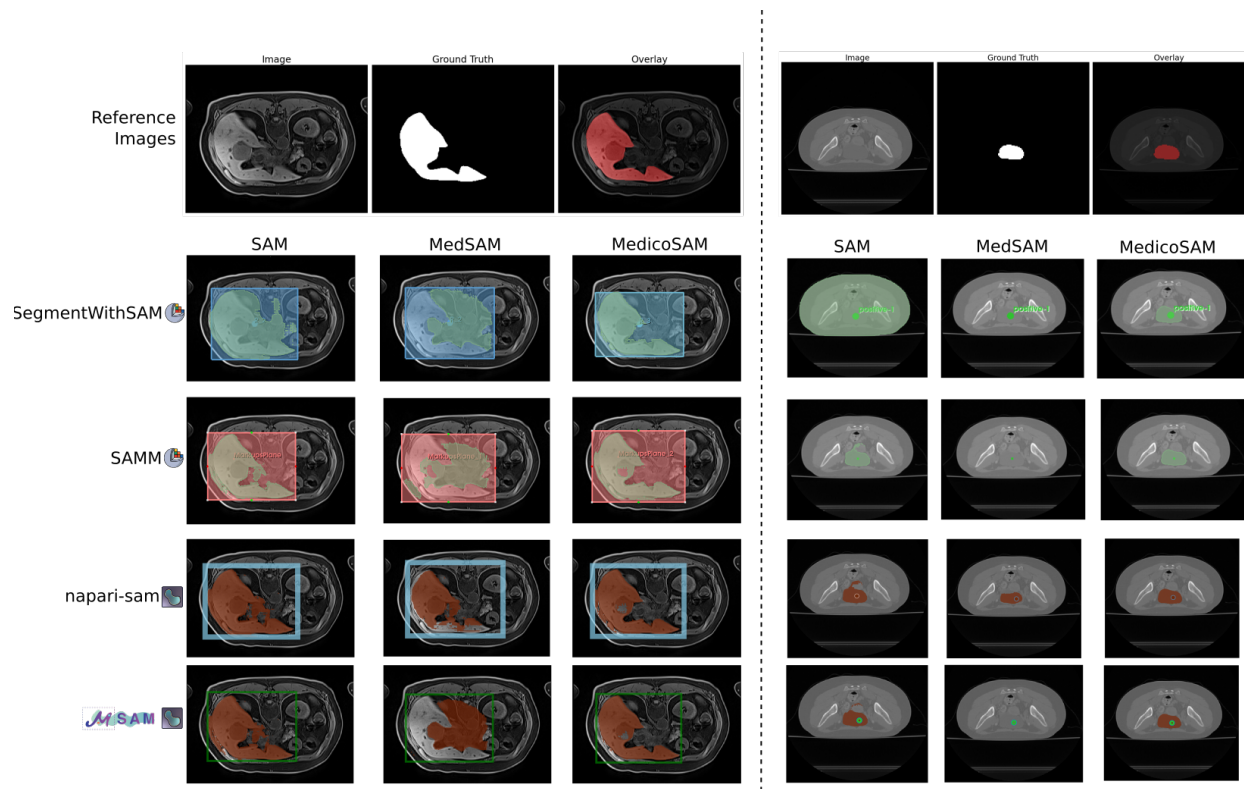


Fig. 6. Using SAM, MedSAM and MedicoSAM in four different tools for interactive segmentation. The top row shows the reference image and the object that is annotated. The four rows below show interactive segmentation results with the different tools. Data on the left hand side shows a section from a abdominal MRI scan [26], the right hand side shows a section from a cervical CT scan [31].

are superior to full parameter updates. Both claims are contrary to our results and may be explained due to different choices in training parameters, including for the nnU-Net baselines, and evaluation datasets. They also study data-efficient finetuning on only 5 training images, which we did not investigate.

We believe that our empirical results will provide valuable context for future efforts to adapt more powerful vision foundation models, e.g. SAM2, to medical images, marking an important step towards building a universal model for medical image segmentation. Besides these empirical findings, we publish our best model, MedicoSAM. It can be easily integrated within existing tools for data annotation. According to our results, it is the best currently available model for interactive segmentation of medical data, and we thus believe that it will provide great practical value.

#### ACKNOWLEDGMENT

The work of Anwai Archit was funded by the Deutsche Forschungsgemeinschaft (DFG, German Research Foundation) - PA 4341/2-1. The work of Luca Freckmann was funded by the DFG under Germany’s Excellence Strategy - EXC 2067/1-390729940. This work was also supported by the Google Research Scholarship “Vision Foundation Models for Bioimage Segmentation”. We gratefully acknowledge the computing time granted by the Resource Allocation Board and provided on the supercomputer Emmy at NHR@Göttingen as part of the NHR infrastructure, under the project nim00007.

We would like to thank Sebastian von Haaren for suggestions on improving data visualizations.

#### REFERENCES

- [1] Anwai Archit et al. “Segment anything for microscopy”. In: *bioRxiv* (2023).
- [2] Federico Bolelli et al. “Tooth fairy: A cone-beam computed tomography segmentation challenge”. In: *MICCAI 2023*.
- [3] Tom Brown et al. “Language models are few-shot learners”. In: *NeurIPS* (2020).
- [4] Nhat-Tan Bui et al. “Sam3d: Segment anything model in volumetric medical images”. In: *arXiv* (2023).
- [5] Fernando Cervantes-Sanchez et al. “Automatic segmentation of coronary arteries in X-ray angiograms using multiscale analysis and artificial neural networks”. In: *Applied Sciences* (2019).
- [6] Cheng Chen et al. “Ma-sam: Modality-agnostic sam adaptation for 3d medical image segmentation”. In: *arXiv* (2023).
- [7] Junlong Cheng et al. “Sam-med2d”. In: *arXiv* (2023).
- [8] Özgün Çiçek et al. “3D U-Net: learning dense volumetric segmentation from sparse annotation”. In: *MICCAI 2016*.
- [9] Noel Codella et al. “Skin lesion analysis toward melanoma detection 2018: A challenge hosted by the international skin imaging collaboration (isic)”. In: *arXiv* (2019).
- [10] Tugba Akinci D’Antonoli et al. “TotalSegmentator MRI: Sequence-Independent Segmentation of 59 Anatomical Structures in MR images”. In: *arXiv* (2024).
- [11] Haoyu Dong et al. “Segment anything model 2: an application to 2d and 3d medical images”. In: *arXiv* (2024).
- [12] Alexey Dosovitskiy et al. “An image is worth 16x16 words: Transformers for image recognition at scale”. In: *arXiv* (2020).

- [13] J Glaister, A Wong, and D A. Clausi. "Automatic segmentation of skin lesions from dermatological photographs using a joint probabilistic texture distinctiveness approach". In: *IEEE Transactions on Biomedical Engineering* (2014).
- [14] Karol Gotkowski. *napari-sam*. Github. 2020.
- [15] Jasper W van der Graaf et al. "Lumbar spine segmentation in MR images: a dataset and a public benchmark". In: *Scientific Data* (2024).
- [16] Hanxue Gu et al. "How to build the best medical image segmentation algorithm using foundation models: a comprehensive empirical study with Segment Anything Model". In: *arXiv* (2024).
- [17] Kaiming He et al. "MAE: Masked autoencoders are scalable vision learners". In: *arXiv* (2021).
- [18] Sheng He et al. "Computer-vision benchmark segment-anything model (sam) in medical images: Accuracy in 12 datasets". In: *arXiv* (2023).
- [19] Nicholas Heller et al. "The state of the art in kidney and kidney tumor segmentation in contrast-enhanced CT imaging: Results of the KiTS19 challenge". In: *MIA* (2021).
- [20] Fabian Hörst et al. "Cellvit: Vision transformers for precise cell segmentation and classification". In: *MIA* (2024).
- [21] Edward J Hu et al. "Lora: Low-rank adaptation of large language models". In: *arXiv* (2021).
- [22] Yuhao Huang et al. "Segment anything model for medical images?" In: *MIA* (2024).
- [23] Fabian Isensee et al. "nnU-Net: a self-configuring method for deep learning-based biomedical image segmentation". In: *Nature methods* (2021).
- [24] Stefan Jaeger et al. "Automatic tuberculosis screening using chest radiographs". In: *IEEE TMI* (2013).
- [25] Wei Ji et al. *Segment anything is not always perfect: An investigation of sam on different real-world applications*. 2024.
- [26] Yuanfeng Ji et al. "Amos: A large-scale abdominal multi-organ benchmark for versatile medical image segmentation". In: *NeurIPS* (2022).
- [27] Hongxu Jiang et al. "MicroSegNet: A deep learning approach for prostate segmentation on micro-ultrasound images". In: *Computerized Medical Imaging and Graphics* (2024).
- [28] Alexander Kirillov et al. "Segment anything". In: *ICCV*. 2023.
- [29] Oleksandr Kovalyk et al. "PAPILA: Dataset with fundus images and clinical data of both eyes of the same patient for glaucoma assessment". In: *Scientific Data* (2022).
- [30] Markus Krönke et al. "Tracked 3D ultrasound and deep neural network-based thyroid segmentation reduce interobserver variability in thyroid volumetry". In: *Plos one* (2022).
- [31] Bennett Landman et al. "Miccai multi-atlas labeling beyond the cranial vault—workshop and challenge". In: *MICCAI 2015*.
- [32] Sarah Leclerc et al. "Deep learning for segmentation using an open large-scale dataset in 2D echocardiography". In: *IEEE TMI* (2019).
- [33] Rebecca Sawyer Lee et al. "A curated mammography data set for use in computer-aided detection and diagnosis research". In: *Scientific data* (2017).
- [34] Wenhui Lei et al. "Medlsam: Localize and segment anything model for 3d medical images". In: *arXiv* (2023).
- [35] Yuheng Li, Mingzhe Hu, and Xiaofeng Yang. "Polyp-sam: Transfer sam for polyp segmentation". In: *Medical Imaging 2024: Computer-Aided Diagnosis*. SPIE. 2024.
- [36] Haofeng Liu et al. "Surgical sam 2: Real-time segment anything in surgical video by efficient frame pruning". In: *arXiv* (2024).
- [37] Yihao Liu et al. "Samm (segment any medical model): A 3d slicer integration to sam". In: *arXiv* (2023).
- [38] I Loshchilov. "Decoupled weight decay regularization". In: *arXiv* (2017).
- [39] Yaosheng Lu et al. "The JNU-IFM dataset for segmenting pubic symphysis-fetal head". In: *Data in brief* (2022).
- [40] Jun Ma et al. "Segment anything in medical images". In: *Nature Communications* (2024).
- [41] Jun Ma et al. "Segment Anything in Medical Images and Videos: Benchmark and Deployment". In: *arXiv* (2024).
- [42] Jacob A Macdonald et al. "Duke Liver Dataset: A publicly available liver MRI dataset with liver segmentation masks and series labels". In: *Radiology: AI* (2023).
- [43] Caroline Magg et al. "Training-free Prompt Placement by Propagation for SAM Predictions in Bone CT Scans". In: *MIDL 2024*.
- [44] Salman Maqbool et al. "m2caiseg: Semantic segmentation of laparoscopic images using convolutional neural networks". In: *arXiv* (2020).
- [45] Daniel S Marcus et al. "Open Access Series of Imaging Studies (OASIS): cross-sectional MRI data in young, middle aged, nondemented, and demented older adults". In: *Journal of cognitive neuroscience* (2007).
- [46] Maciej A Mazurowski et al. "Segment anything model for medical image analysis: an experimental study". In: *MIA* (2023).
- [47] Cancer Genome Atlas Research Network. "Comprehensive, integrative genomic analysis of diffuse lower-grade gliomas". In: *New England Journal of Medicine* (2015).
- [48] Antonio Pepe, Gian Marco Melito, and Jan Egger. "Segmentation of the Aorta: Towards the Automatic Segmentation, Modeling, and Meshing of the Aortic Vessel Tree from Multicenter Acquisition". In: *MICCAI 2023* ().
- [49] Gašper Podobnik et al. "HaN-Seg: The head and neck organ-at-risk CT and MR segmentation dataset". In: *Medical physics* (2023).
- [50] Nikhila Ravi et al. "Sam 2: Segment anything in images and videos". In: *arXiv* (2024).
- [51] Julio César Mello Román et al. "Panoramic dental radiography image enhancement using multiscale mathematical morphology". In: *Sensors* (2021).
- [52] Olaf Ronneberger, Philipp Fischer, and Thomas Brox. "U-net: Convolutional networks for biomedical image segmentation". In: *MICCAI 2015*.
- [53] Luisa F Sánchez-Peralta et al. "Piccolo white-light and narrow-band imaging colonoscopic dataset: A performance comparative of models and datasets". In: *Applied Sciences* (2020).
- [54] Ahmed Shahin et al. *OSIC Pulmonary Fibrosis Progression*. Kaggle. 2020.
- [55] Ashish Vaswani et al. "Attention is all you need". In: *NeurIPS* (2017).
- [56] Haoyu Wang et al. "SAM-Med3D". In: *arXiv preprint* (2023).
- [57] Jakob Wasserthal et al. "TotalSegmentator: robust segmentation of 104 anatomic structures in CT images". In: *Radiology: AI* (2023).
- [58] Junde Wu et al. "Medical sam adapter: Adapting segment anything model for medical image segmentation". In: *arXiv* (2023).
- [59] Jin Ye et al. "Sa-med2d-20m dataset: Segment anything in 2d medical imaging with 20 million masks". In: *arXiv* (2023).
- [60] Xin Ye et al. "OIMHS: An Optical Coherence Tomography Image Dataset Based on Macular Hole Manual Segmentation". In: *Scientific Data* (2023).
- [61] Zafer Yildiz et al. "SegmentWithSAM: 3D Slicer Extension for Segment Anything Model (SAM)". In: *MIDL 2024*.
- [62] Wenxi Yue et al. "Surgicalsam: Efficient class promptable surgical instrument segmentation". In: *AAAI Conference on Artificial Intelligence*. 2024.
- [63] Anna Zawacki et al. *SIIM-ACR Pneumothorax Segmentation*. Kaggle. 2019.
- [64] Kaidong Zhang and Dong Liu. "Customized segment anything model for medical image segmentation". In: *arXiv* (2023).
- [65] Jiayuan Zhu, Yunli Qi, and Junde Wu. "Medical sam 2: Segment medical images as video via segment anything model 2". In: *arXiv* (2024).

## APPENDIX

We show qualitative comparisons of interactive 2D and 3D segmentation with SAM, MedSAM and MedicoSAM.

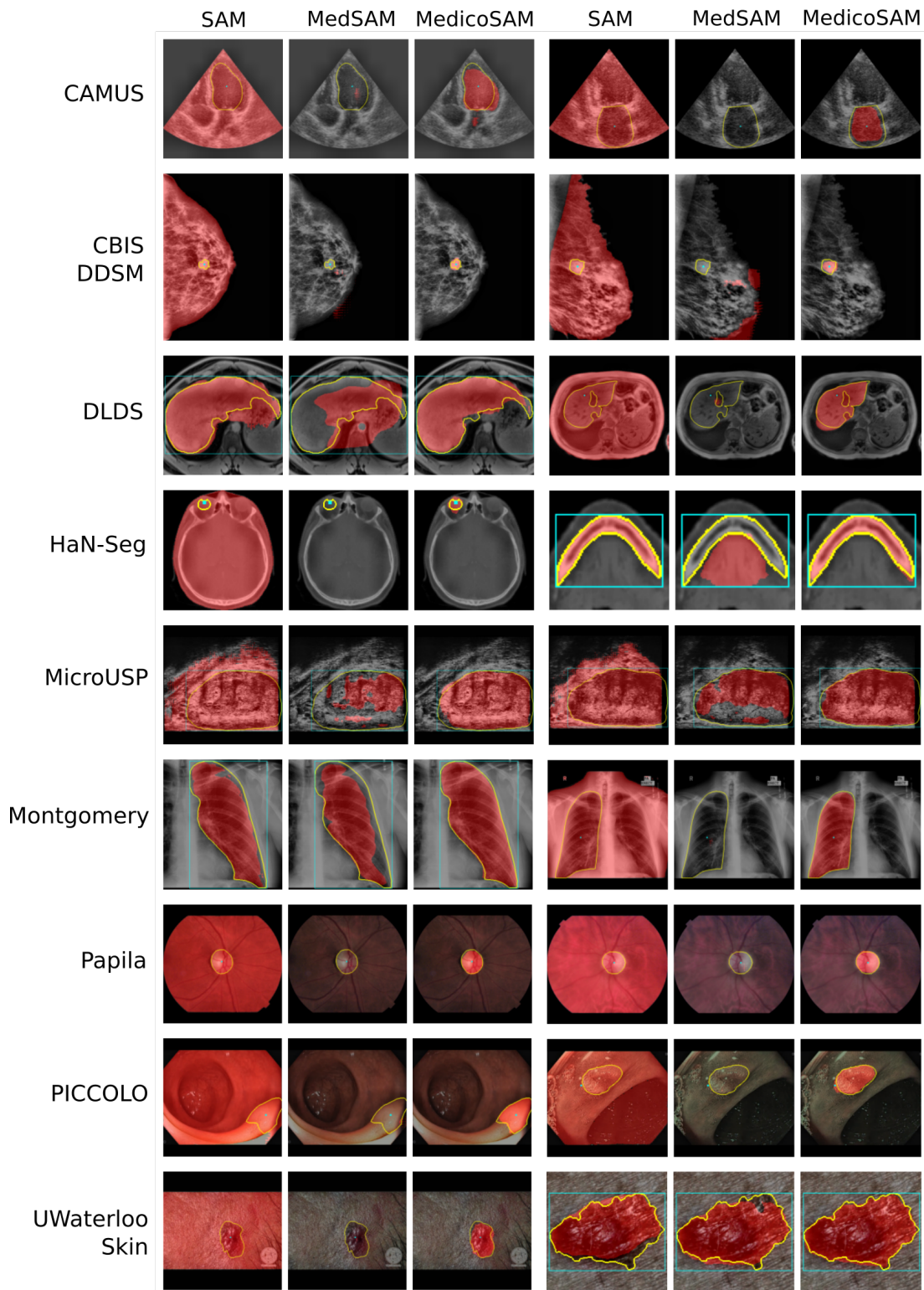
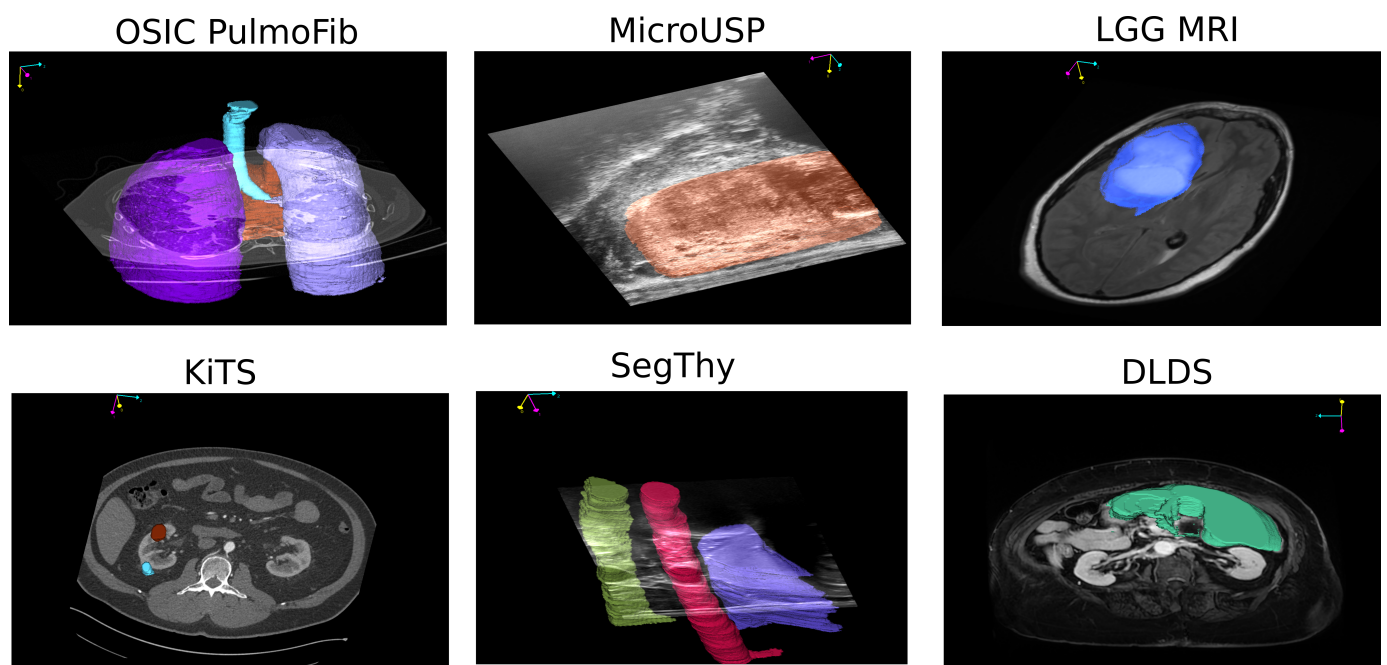


Fig. 7. Qualitative results for interactive 2D segmentation. We compare interactive segmentation based on a single point or single box prompt (cyan) with SAM, MedSAM, and MedicoSAM for nine different datasets. For each image, we show prompts with a large improvement of MedicoSAM over SAM and the corresponding MedSAM result. Note that the quantitative results in Fig. 3 show overall improved segmentation with MedicoSAM.



**Fig. 8.** Qualitative results for interactive 3D segmentation. We show rendered 3D segmentations for objects in the volume that were segmented from a single prompt with MedicoSAM.